International Journal of Geometric Methods in Modern Physics
Vol. 20, No. 4 (2023) 2350058 (28 pages)

DOI: 10.1142/S0219887823500585

On evolution of compact stars from string fluid in Rastall gravity

Umber Sheikh*

Division of Science and Technology
Department of Mathematics
University of Education, Lahore, Pakistan
umber.sheikh@ue.edu.pk

Yousra Aziz

Department of Applied Sciences
National Textile University, Faisalabad, Pakistan
azizyousra2@gmail.com
2019ntumsmm3025@ntu.edu.pk

M. Z. Bhatti

Department of Mathematics, University of the Punjab
Quaid-i-Azam Campus, Lahore, Pakistan
mzaeem.math@pu.edu.pk

Richard Pincak

Institute of Experimental Physics
Slovak Academy of Sciences, 04011 Košice, Slovakia
pincak@saske.sk

Received 28 July 2022
Accepted 9 October 2022
Published 29 November 2022

The aim of this work is to discuss the evolution of compact stars from the view point of a string fluid in Rastall theory using Krori–Barua (KB) metric as interior geometry. The exterior spacetime is considered as Schwarzschild metric while matching of interior and exterior spacetimes lead to coefficients of KB ansatz. The field equations and dynamical variables of the string fluid are explored. We found the values of Rastall parameter η for which the dynamical variables satisfy the energy conditions which shows the existence of physical matter. The model is applied to specific physical features including energy conditions, anisotropy, stability, Tolman–Oppenheimer–Volkoff equation, mass function, compactness and redshift of compact stars, in particular, SAX J1808.4-3658, Vela X-12 and Hercules X-1. It is found that the presented model fulfills all the physical requirements

*Corresponding author.

and thus, is realistic. We conclude that the string fluid is responsible for the evolution of compact stars in the cosmos.

Keywords: Compact stars; Rastall theory of gravity; anisotropy; stability.

PACS: 04.40 Dg, 04.50 Kd, 75.30 Gw

1. Introduction

A compact star is a massive object within a relatively small volume compared to an ordinary star. It is a collapsed star with an outer core of the degenerate matter and has a strong gravitational field. Such stars include white dwarfs, neutron stars and black holes. After the stellar death, the residue may become a compact star. Compact objects are the test center to investigate various properties of their immense gravitational field [1, 2]. A close examination of the ages, structures and evolution of compact stars as well as their astrophysical properties is a subject of interest in cosmology [3–5].

The theoretical structural and physical predictions concerning a compact object depends on their line element. The line element provides comprehensive information about the formation of compact stars [6]. The Krori–Barua (KB) spacetime is the best for the description of compact stars including strange and hybrid stars [7, 8].

Rastall theory is the extended theory of gravity that inculcates cosmological problems like Hubble's parameter, age of the Universe, description of matter dominant and other cosmic eras, and gravitational lensing phenomena. The observational data regarding many cosmological problems agree with the results of Rastall theory [9, 10]. The theory explains various cosmological phenomena and provides promising results in a non-conserved background.

Rastall theory admits a non-minimal coupling of gravity with the energy–momentum source. Thus, it encapsulates the description of quantum features including particle creation which is a factor of the violation of matter conservation law. Moreover, the field equations of Rastall theory are simpler compared to those of other curvature–matter theories. Thus, astronomical phenomena are consequently easier to investigate. As an extended theory of gravity, Rastall theory discusses the compact, quark and neutron stars [11, 12]. Solution to the isotropic and anisotropic compact star models under specific circumstances lead to different models of compact and strange stars [13, 14].

The formation of compact stars gained interest in alternative theories of gravity. The $f(R)$ theories of gravity discuss the physical viability, regularity, stability, and equilibrium, and energy conditions of the anisotropic compact stars. The theoretical results are validated via astronomical observations from SAX J1808.4-3658, Cen X-3, Swift J1818.0-1607, 4U1820-30, EXO 1785-248, PSR J1614-2230, LMC X-4, SMC X-1, Her X-I and PSR J0348+0432 [15–18]. The anisotropy of the system, anisotropic stress, speed of sound, adiabatic constant, equilibrium and energy conditions, surface redshift, electric intensity, compactness factor and stability of these stars is a hot topic in $f(T)$ theory. The dynamical instability of cylindrically symmetric models is also explored [19]. The dynamical quantities, energy, causality and stability conditions and other physical properties of compact stars and strange stars are investigated and validated for Vela X-1, PSR J1614-2230, Cen X-3 and SAX J1808.4-3658 in $f(R,T)$ gravity [20–22]. The configuration of compact stars and their physical aspects including density, pressure and stress variations, different forces of equilibrium, stability, anisotropy, equation of state parameters and charge distribution are modeled in $f(G)$, $f(G,T)$, $f(T,T)$ and $f(R,G)$ theories of gravity. The results are validated with the observational data from Cen X-3, EXO 1785-248, LMC X-4, SAX J1808.4-3658, PSR 1937+21, PSR J1903+327, PSR J1614-2230, 4U1820-30, 4U1538-52 and Her X-1 [23–27]. A significant theory to discuss the energy, linear and angular momentum, casualty, stability, Killing vectors and inflation is the theory of teleparallel gravity [28–34]. This theory deals with torsion instead of curvature. This theory also interprets singularities, charged and uncharged compact structures [35–38]. The compact and strange stars have also been of great interest in theories of Brans–Dickey gravity, Einstein–Gauss–Bonnet gravity and Energy–Momentum squared gravity [3, 39, 40].

The string-oriented fluids are interesting to study in the scenario of gravitational collapse. The collapse of a string fluid in cylindrical spacetime exhibits the effect of charge on the relativistic model [41]. The dynamics of collapsing uncharged and charged string dust [42, 43] and string fluid [44, 45] gives an insight of the black hole information paradox in the theory of rainbow gravity. All the results exhibit that the black hole event horizon depends on the energy of the particle. Thus, a particle with higher energy level can take the information from a particle with lower energy level which resolves the information paradox. The collapsing string fluid in conjunction with null radiation has piqued the curiosity of general relativity [46,47]. Strings are the one-dimensional vibrating filaments of energy. Strings encompass the quantum characteristics in the relativistic dynamic spacetime with fluid. The study of string-oriented fluids aids in understanding quantized gravity and unification of all natural forces [48]. The simplest string-oriented model is the string dust, the string-oriented incoherent matter particles. By applying an isotropic pressure on the string dust, a basic model of string fluid emerges that is a perfect fluid oriented with strings.

This paper is devoted to modeling the dynamics of a compact star rising from collapsing radially anisotropic string fluid in Rastall theory of gravity. In Sec. 2, the KB spacetime is considered to model interior of a compact star. The field equations of Rastall gravity are modified considering the presence of radially anisotropic perfect fluid. The dynamical variables are evaluated and represented graphically. Section 3 comprises the exterior line element and matching conditions. Section 4 consists of the requirements of a physical model and graphical representation of physical features for the existence of compact stars is done. The model is validated using the observational data of SAX J1808.4-3658, Vela X-1 and Hercules X-1. Section 5 contains the conclusion.

2. Geometry of Spacetime and Fluid Description

In this section, we will describe the geometry of interior and exterior spacetime for a systematic investigation of our analysis. The interior spacetime is taken to be KB metric representing a non-singular spacetime, whereas the exterior spacetime is the Schwarzschild metric. The line element of interior and exterior spacetimes can be written, respectively, as [7]

$$ds_-^2 = -e^{\gamma(r)}dt^2 + e^{\mu(r)}dr^2 + r^2(d\theta^2 + \sin^2\theta d\phi^2), \tag{1}$$

$$ds_+^2 = -(1-2Mr^{-1})dt^2 + (1-2Mr^{-1})^{-1}dr^2 + r^2(d\theta^2 + \sin^2\theta d\phi^2). \tag{2}$$

The interior spacetime (KB spacetime) in Eq. (1) contains $\gamma(r) = Qr^2 + C$ and $\mu(r) = Lr^2$ where $L,\ Q,\ C$ are arbitrary coefficients and can be determined from the matching conditions. Assuming that both the interior and exterior spacetimes meet at the boundary $r = R$, where the metric coefficients of $g_{tt},\ g_{rr}$ and $\frac{\partial g_{tt}}{\partial r}$ are all continuous, one obtains the following relations:

$$1 - 2MR^{-1} = e^{\gamma(r)} \Rightarrow 1 - 2MR^{-1} = e^{QR^2+C}, \tag{3}$$

$$(1 - 2MR^{-1})^{-1} = e^{\mu(r)} \Rightarrow (1 - 2MR^{-1})^{-1} = e^{LR^2}, \tag{4}$$

$$MR^{-2} = \gamma' e^{\gamma(r)} \Rightarrow MR^{-2} = QRe^{QR^2+C}. \tag{5}$$

It is interesting to note that the derivatives of g_{tt} and g_{rr} with respect to time needed to be continuous at the junction. Moreover, the derivative $\frac{\partial g_{rr}}{\partial r}$ need not to be continuous at the surface [49].

Equations (3)–(5) lead to the following values of the arbitrary coefficients:

$$L = -R^{-2}\ln(1-2MR^{-1}), \quad Q = MR^{-3}(1-2MR^{-1})^{-1},$$
$$C = \ln(1-2MR^{-1}) - MR^{-1}(1-2MR^{-1})^{-1}. \tag{6}$$

To model a compact object graphically, we need suitable values of KB coefficients, $L,\ Q$ and C. For the sake of validation of our model, we take three candidates for compact stars with the following observational data [50, 51].

The interior spacetime (KB spacetime) admits the existence of a string fluid with the following matter tensor [41]:

$$T_{\mu\nu} = (\rho + p)u_\mu u_\nu + pg_{\mu\nu} - \lambda x_\mu x_\nu, \tag{7}$$

Table 1. The masses $M\,(M_\odot)$, radii $R\,$(km) and the constants L and Q for the compact stars SAX J1808.4-3658, Vela X-12 and Hercules X-1.

Compact star	M	R	L	Q
SAX J1808.4-3658	1.435	7.07	$1823156974 \times 10^{-11}$	$14880115690 \times 10^{-12}$
Vela X-12	1.77	9.99	$741034129 \times 10^{-11}$	$5485958565 \times 10^{-12}$
Hercules X-1	0.88	7.7	$690627643 \times 10^{-11}$	$4267364618 \times 10^{-12}$

where ρ is the matter density, p is the pressure of fluid, $g_{\mu\nu}$ is metric tensor and λ is the string tension. The vectors u_μ, x_μ, respectively, represent the velocity and radial position vectors with

$$-u^\mu u_\mu = x^\mu x_\mu = 1.$$

It is noteworthy that

- When $p = 0$, Eq. (7) shows a string cloud.
- When $l = 0$, Eq. (7) exhibits a perfect fluid.
- The fluid is stiff for $\rho - p = 0$ and anti-stiff for $\rho + p = 0$.
- The strings are Reddy for $\rho + l = 0$ or Nambu for $\rho - l = 0$.

3. Field Equations of Rastall Gravity and Dynamical Variables

We shall explore the Rastall field equations for an anisotropic matter distribution known as the string fluid. Rastall theory deals with the non-conservation of energy–momentum, i.e. $T^{\mu\gamma}_{;\mu} = 0$ as [9]

$$T^{\mu\nu}_{;\mu} = \eta R^{,\nu}, \tag{8}$$

where η is Rastall's dimensionless parameter which shows the digression from general relativity as well as the relation between matter field and geometry. Thus, the field equations in Rastall gravity turn out to be

$$G_{\mu\nu} + \eta g_{\mu\nu} R = \kappa T_{\mu\nu}. \tag{9}$$

Here, κ, R and $T_{\mu\nu}$ represent gravitational coupling constant, Ricci scalar and energy–momentum tensor, respectively. This equation leads to $R(4\eta - 1) = T$, and thus [9]

$$\kappa = 8\pi \frac{4\eta - 1}{6\eta - 1}.$$

Consequently, the field equations in the Rastall framework can be written as

$$G_{\mu\nu} + \eta\, g_{\mu\nu} R = 8\pi \left(\frac{4\eta - 1}{6\eta - 1}\right) T_{\mu\nu}. \tag{10}$$

It is noteworthy that $\eta = \frac{1}{6}$ and $\eta = \frac{1}{4}$ are not permissible. The value $\eta = \frac{1}{6}$ makes the right-hand side of Eq. (10) infinite. This indicates an infinite matter and hence, infinite energy inside the star. This leads to the concept of infinite energy which is not possible inside the star's structure. Moreover, the value of the Rastall parameter $\eta = \frac{1}{4}$ makes the right-hand side of Eq. (10) vanishing. This indicates a vacuum inside the star. Both these situations are not physical. Moreover, $\eta = 0$ leads to the Einstein field equations of general relativity. Substituting the metric from the interior spacetime (KB spacetime), Eq. (1) and energy–momentum tensor of string fluid Eq. (7), the field equations from Eq. (10) yield

$$8\pi\rho\left(\frac{4\eta-1}{6\eta-1}\right)=e^{-\mu}\left[\frac{e^{\mu}-1}{r^2}+\frac{\mu'}{r}+\eta\left\{\gamma''-\mu'\gamma'+\gamma'^2-\frac{2}{r}(\mu'-\gamma')\right.\right.$$
$$\left.\left.-\frac{2}{r^2}(e^{\mu}-1)\right\}\right], \tag{11}$$

$$8\pi(p-\lambda)\left(\frac{4\eta-1}{6\eta-1}\right)=e^{-\mu}\left[\frac{1-e^{\mu}}{r^2}+\frac{\gamma'}{r}-\eta\left\{\gamma''-\mu'\gamma'+\gamma'^2-\frac{2}{r}(\mu'-\gamma')\right.\right.$$
$$\left.\left.-\frac{2}{r^2}(e^{\mu}-1)\right\}\right], \tag{12}$$

$$8\pi p\left(\frac{4\eta-1}{6\eta-1}\right)=e^{-\mu}\left[\frac{-\mu'\gamma'r+\gamma'^2r+2\gamma''r-2\mu'+2\gamma'}{4r}\right.$$
$$\left.-\eta\left\{\gamma''-\mu'\gamma'+\gamma'^2-\frac{2}{r}(\mu'-\gamma')-\frac{2}{r^2}(e^{\mu}-1)\right\}\right], \tag{13}$$

where prime indicates the derivative corresponding to the radial coordinate. It is obvious that in this system of equations, there are three dynamical unknowns, the matter density ρ, pressures p and string tension λ. It is noteworthy that Eqs. (11) and (13) directly give the expressions for mass density ρ and pressure p. The value of string tension λ can be obtained subtracting Eq. (12) from Eq. (13). A handsome use of KB ansatz leads to the following expressions for the dynamical variables:

$$\rho=\frac{e^{-Lr^2}}{8\pi}\left[\frac{e^{Lr^2}-1}{r^2}+2L+\eta\{(2Q+4Qr^2(Q-L)-4(L-Q)-\frac{2}{r^2}(e^{Lr^2}-1)\}\right]$$
$$\times\left(\frac{6\eta-1}{4\eta-1}\right), \tag{14}$$

$$p=\frac{e^{-Lr^2}}{8\pi}\left[Qr^2(Q-L)+2Q-L-\eta(2Q+4Qr^2(Q-L)-4(L-Q)\right.$$
$$\left.-\frac{2}{r^2}(e^{Lr^2}-1))\right]\left(\frac{6\eta-1}{4\eta-1}\right), \tag{15}$$

$$\lambda=\frac{e^{-Lr^2}}{8\pi}\left[\frac{e^{Lr^2}-1}{r^2}+Qr^2(Q-L)+4Q-L\right]\left(\frac{6\eta-1}{4\eta-1}\right). \tag{16}$$

The physical features including matter density, pressure and string tension of the model can be validated considering different values of Rastall parameter η. The existence of a physical fluid requires the satisfaction of null energy condition (NEC), weak energy condition (WEC) and strong energy condition (SEC). All the energy

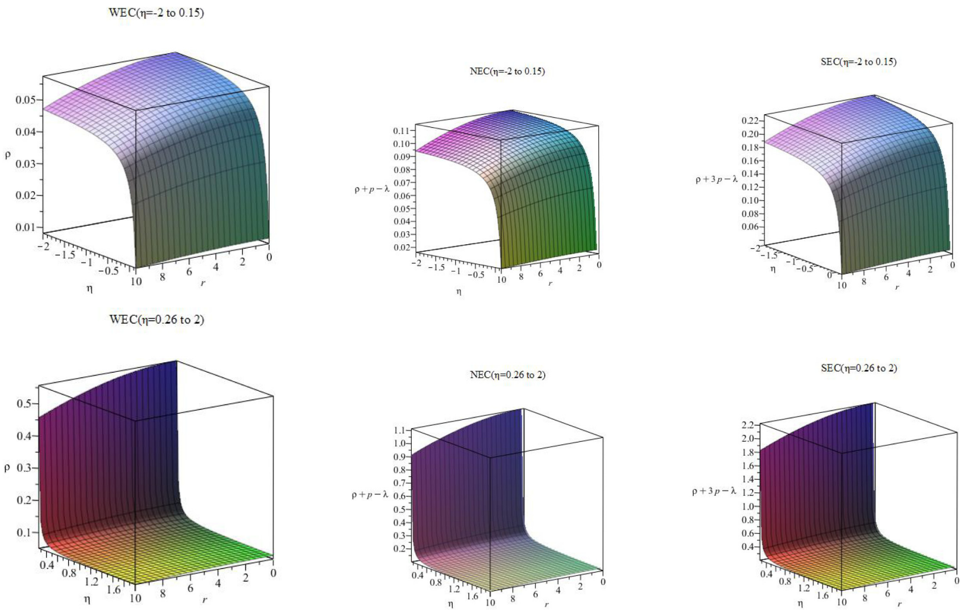

Fig. 1. WEC, NEC and SEC for Rastall's dimensionless parameter $\eta < \frac{1}{6}$ and $\frac{1}{4} > \eta$.

conditions insist that energy must be positive because negative energy never leads to a stable configuration. The energy conditions for a string fluid are [41]:

- **WEC:** The WEC for the string fluid is $\rho > 0$.
- **NEC:** The NEC for the string fluid is $\rho + p - \lambda > 0$.
- **SEC:** The SEC for the string fluid is $\rho + 3p - \lambda > 0$.

It is noteworthy that all these energy conditions are satisfied for the values of Rastall parameter $\eta < \frac{1}{6}$ and $\eta > \frac{1}{4}$.

Figure 1 illustrates that all the energy conditions are satisfied for all the radial values and regions $\eta < \frac{1}{6}$ and $\eta > \frac{1}{4}$ for Rastall dimensionless parameter. Now, we shall observe the behavior of the dynamical variables of the string fluid for the valid regions of the Rastall dimensionless parameter $\eta < \frac{1}{6}$ and $\eta > \frac{1}{4}$.

Figure 2 demonstrates the behavior of mass density ρ of the fluid corresponding to the radius r and Rastall's dimensionless parameter η. It is obvious that the mass density ρ increases as the radius r of the sphere decreases. Towards the center of the compact star $r = 0$, the matter gets denser which is a physical phenomenon. Moreover, the mass density decreases as Rastall's dimensionless parameter η increases.

Figure 3 illustrates the behavior of pressure p of the fluid corresponding to the radius r and Rastall's dimensionless parameter η. The pressure of the fluid p increases as the radius r of the sphere decreases. Towards the center of the compact star $r = 0$, the pressure of the fluid increases due to an increase in matter density,

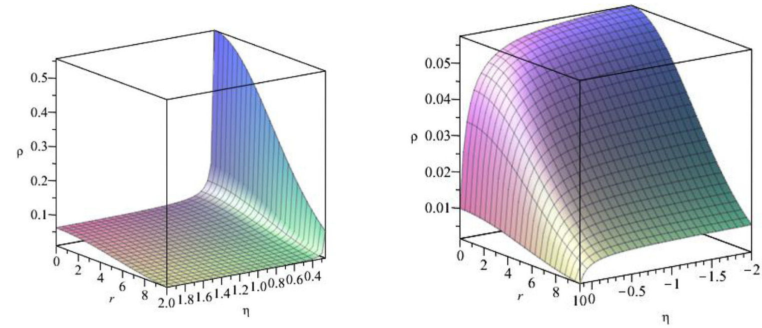

Fig. 2. Variation of mass density ρ with respect to radius r and Rastall's dimensionless parameter $\eta < \frac{1}{6}$ and $\frac{1}{4} > \eta$.

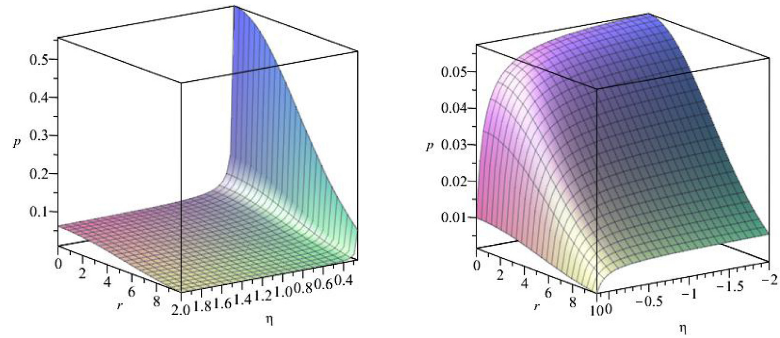

Fig. 3. Variation of tangential pressure p with respect to radius r and Rastall's dimensionless parameter $\eta < \frac{1}{6}$ and $\frac{1}{4} > \eta$.

which is a physical phenomenon. Also, the fluid's pressure decreases as Rastall's dimensionless parameter η increases.

Figure 4 shows the variation of radial pressure $p - \lambda$ with respect to the radius r and Rastall dimensionless parameter η. The radial pressure of the fluid $p - \lambda$ decreases as the radius r of sphere increases. This indicates a maximum pressure of fluid near the center $r = 0$ which is a physical phenomenon. Moreover, $p - \lambda$ decreases as Rastall's dimensionless parameter η increases.

Figure 5 shows the behavior of string tension λ of the fluid corresponding to the radius r and Rastall's dimensionless parameter η. The string tension λ increases as the radius r of the sphere decreases. Moreover, the string tension λ decreases as Rastall's dimensionless parameter η increases.

For the physically acceptable configuration of a compact star, the mass density and pressure should be

(1) positive throughout the fluid sphere;
(2) regular and non-singular inside the fluid sphere;

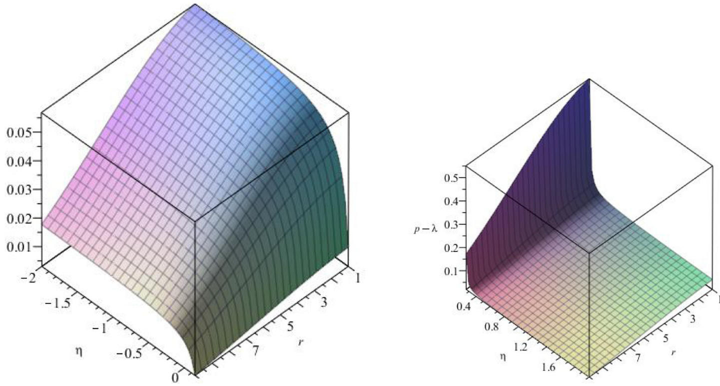

Fig. 4. Variation of radial pressure $p - \lambda$ with respect to radius r and Rastall's dimensionless parameter $\eta < \frac{1}{6}$ and $\frac{1}{4} > \eta$.

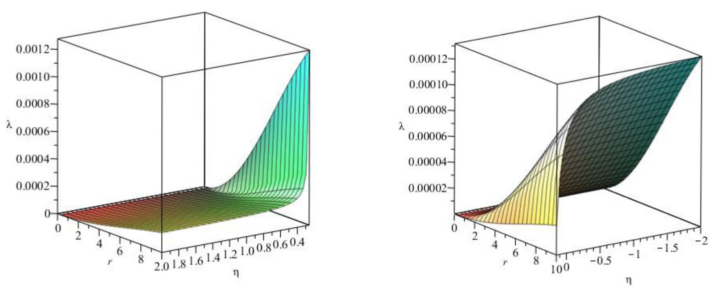

Fig. 5. Variation of string tension λ with respect to radius r and Rastall's dimensionless parameter $\eta < \frac{1}{6}$ and $\frac{1}{4} > \eta$.

(3) attain their maximum values at the origin and decrease gradually towards the surface of the star.

All these conditions are clearly satisfied in Figs. 2–5.

4. Physical Features of the Model

This section is devoted to investigate various physical features of relativistic compact stellar structure. These include energy conditions, stability, Tolman–Oppenheimer–Volkoff (TOV) equation, mass function, compactness and surface redshift. These physical features are calculated for SAX J1808.4-3658, Vela X-12 and Hercules X-1 using data (R, L and Q) given in Table 1.

4.1. *Energy conditions*

The physical solution of the dynamical variables of the fluid is subject to the existence of physical matter in the collapsing body. This is ensured by the satisfaction

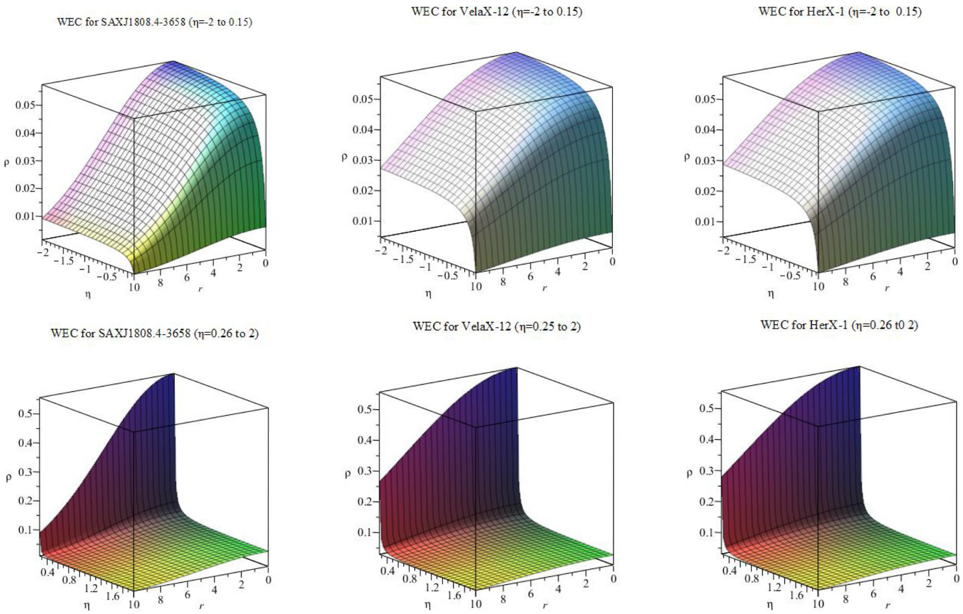

Fig. 6. WEC for SAX J1808.4-3658, Vela X-12 and Hercules X-1.

of energy conditions of the collapsing fluid. These include NEC, WEC and SEC. The NEC narrates that the stress energy encountered by a light beam must not be negative. The WEC states that the local mass–energy density cannot be negative. The SEC states that matter is compelled to be attracted toward other matter.

A physical string fluid configuration requires the energy conditions WEC $\rho > 0$, NEC $\rho + p - \lambda > 0$, SEC $\rho + 3p - \lambda > 0$, to be satisfied by the matter inside it. All these energy conditions are satisfied for the models of SAX J1808.4-3658, Vela X-12 and Hercules X-1 in Figs. 6–8.

4.2. *Effect of anisotropy*

Anisotropy in fluid's pressure usually arises due to presence of mixture of different types of fluids, magnetic field or external field, rotation, existence of super fluid, viscosity and phase transitions. The anisotropy parameter represents a repulsive force which prevents the compact celestial body from further collapse. It is noteworthy that the increasing anisotropic parameter represents the zones of greater stability. The anisotropy parameter Δ is calculated using Eqs. (12) and (13). The following scenarios are possible:

- When $\Delta > 0$, the anisotropic force is repulsive and directed outward.
- When $\Delta = 0$, there would be no anisotropic force.
- When $\Delta < 0$, the anisotropic force is attractive in nature and inward directed.

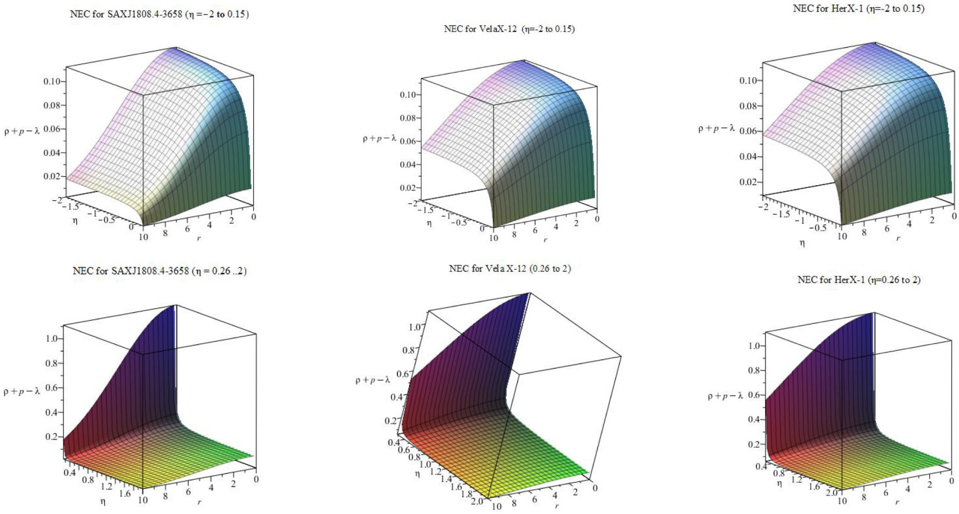

Fig. 7. NEC for SAX J1808.4-3658, Vela X-12 and Hercules X-1.

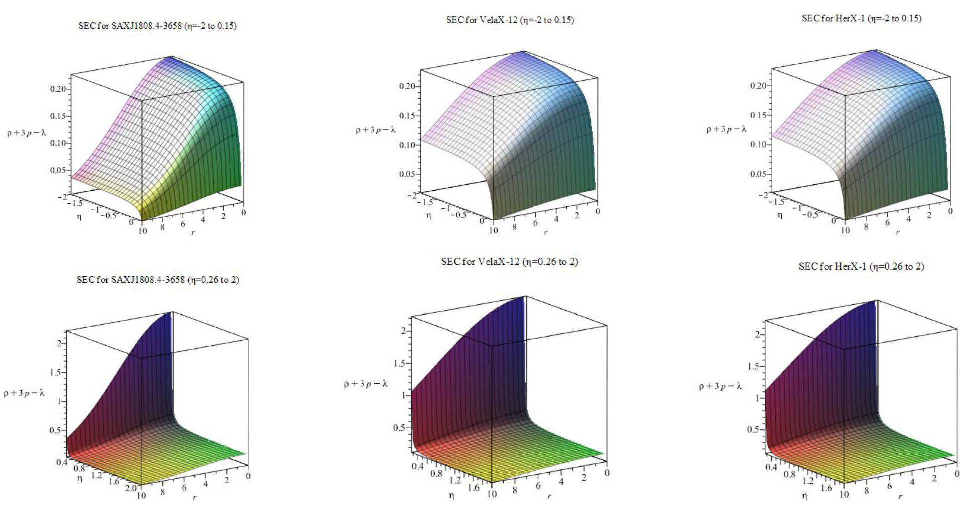

Fig. 8. SEC for SAX J1808.4-3658, Vela X-12 and Hercules X-1.

The variations of the anisotropy parameter Δ for the defined model is exhibited in Fig. 9.

Figure 9 indicates that there anisotropy vanishes at the center $r = 0$ of the configuration. It gradually boosts from the center towards the outer (boundary) surface of the star. The positive anisotropy leads our model to achieve a stable configuration. The same behavior is exhibited in Fig. 10 by the compact stars SAX J1808.4-3658, Vela X-12 and Hercules X-1.

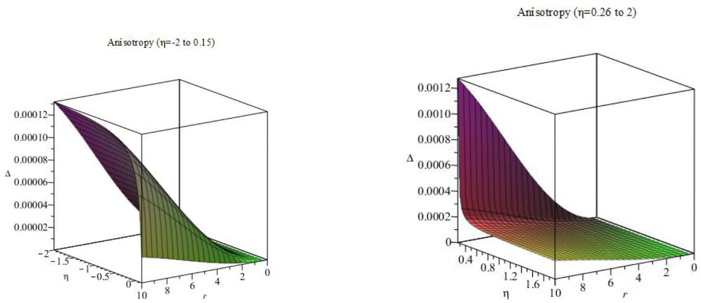

Fig. 9. Variation of anisotropy parameter Δ with respect to radius r and Rastall's dimensionless parameter $\eta < \frac{1}{6}$ and $\frac{1}{4} > \eta$.

4.3. *Stability analysis*

The stable compact objects are more significant as they are more realistic and physical. The capacity of an object to get its stabilized position under the implementation of force is called stability. After the dynamical fluctuations, the stable stellar bodies are worthwhile to study. According to Herrera's cracking condition [52], in a stable stellar structure, the square of speed of sound in the fluid, estimated from the formula $v_s^2 = \frac{dp}{d\rho}$ should lie $0 \leq v_s^2 \leq 1$. For the string fluid, the squared speed

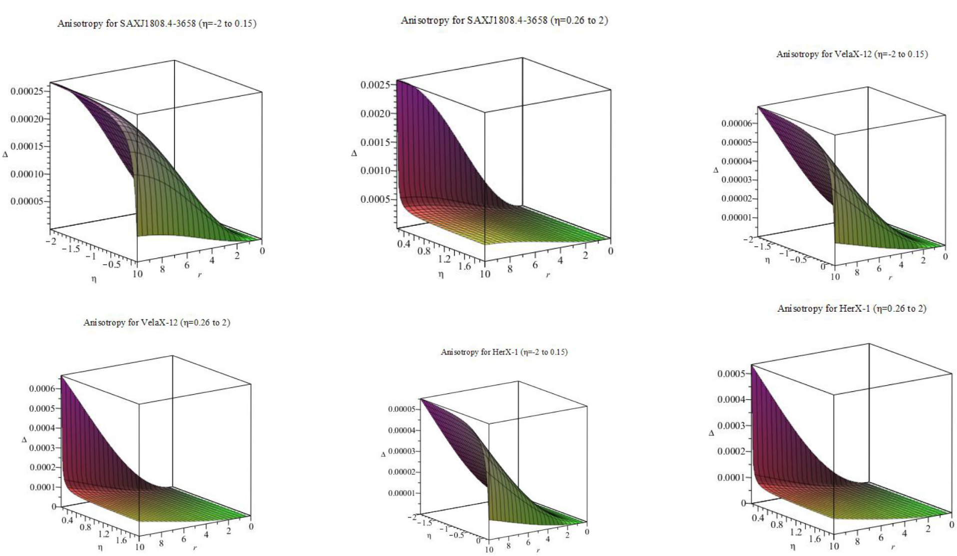

Fig. 10. Variation of anisotropy parameter Δ for compact star candidates SAX J1808.4-3658, Vela X-12 and Hercules X-1.

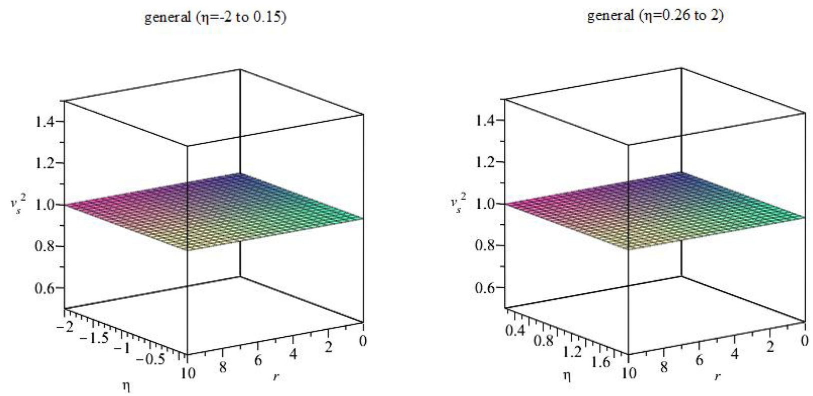

Fig. 11. Variation of squared speed of sound with respect to radius r and Rastall's dimensionless parameter $\eta < \frac{1}{6}$ and $\frac{1}{4} > \eta$.

of sound can be estimated using the following formula:

$$v_s^2 = \frac{dp}{d\rho} = \frac{dp}{dr} \times \frac{dr}{d\rho} = \frac{\begin{pmatrix} 2Q(Q-L)(1-Lr^2)(4\eta-1) \\ \quad + 4LQ\{1-\eta(1+2r^2(Q-L)+2)\} \\ \quad - 2L^2(1-4\eta) + \frac{4}{r^2}\left(\frac{1}{r^2 e^{-Lr^2}} - L - \frac{1}{r^2}\right) \end{pmatrix}}{\frac{4}{r^2}\left(\frac{1}{r^2 e^{-Lr^2}} - L - \frac{1}{r^2}\right)}. \tag{17}$$

For our model, the squared speed of sound is illustrated in the following figure.

Figure 11 indicates that the speed of sound is unity for all radial values r as well as all values of Rastall parameter η for any generalized model. It is possible that the matter sound speed is the same as the speed of light [53], i.e. $c_s^2 = \frac{dp}{d\rho} = c^2$. This is the case of maximum mass neutron star. The squared speed of sound for anisotropic configuration of the three models SAX J1808.4-3658, Vela X-12 and Hercules X-1 is shown in Fig. 12.

All the figures indicate that the speed of sound is unity for all radial values r as well as for all values of Rastall parameter η. This elaborates that all the models are stable.

4.4. *TOV equation and equilibrium conditions*

The equilibrium is a condition or state in which the physical forces are balanced. The equilibrium condition confirms the final state of a compact object that it will not go through further collapse or turn to any other object. The stable state of matter

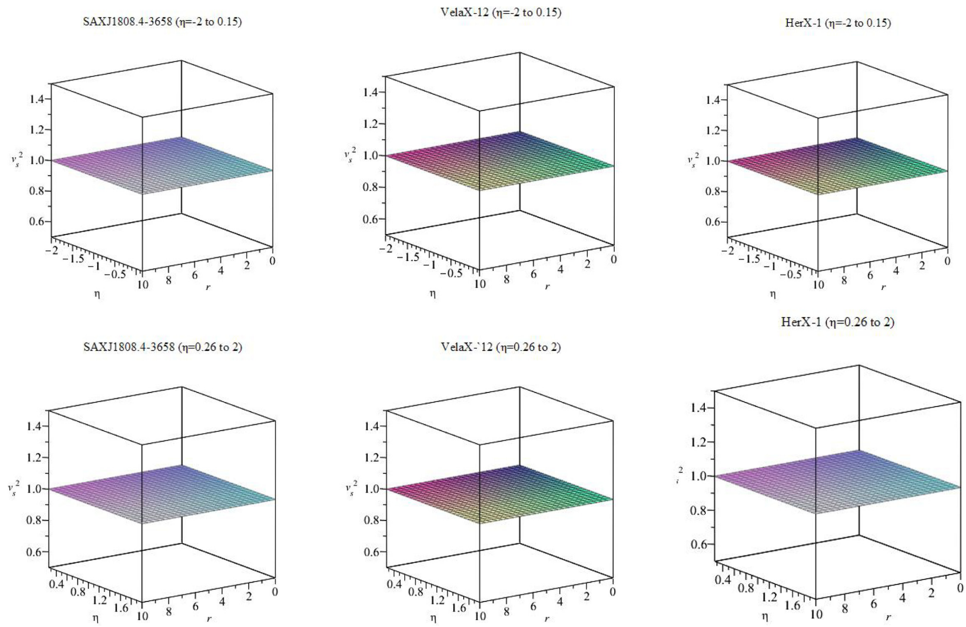

Fig. 12. Variation of squared speed of sound for compact star candidates SAX J1808.4-3658, Vela X-12 and Hercules X-1.

composition in Rastall theory of gravity can be estimated using the generalized TOV equation obtained from non-conservation of the energy–momentum tensor (Eq. (8)) as [58, 59]

$$\left(\frac{\eta}{4\eta-1}\right)\frac{d}{dr}(\rho-3p+\lambda)+\frac{2}{r}\lambda-\frac{(\gamma)'}{2}(\rho+p)-\frac{dp}{dr}=0. \tag{18}$$

The TOV equation gives the full description of the gravitational, mechanical and hydrodynamical properties of general relativistic stars. The required input is the form of matter tensor for the interior of the star which provides a simple and effective description of the main features of spherical symmetric structure. The dynamics of a star's interior is difficult to interpret due to the bulk properties, oscillations, stability and radiations which are all collectively interpreted as TOV equation.

The TOV equation plays a crucial role in calculating the mass and radius of compact objects. This is the equation for the star's hydrostatic equilibrium, meaning that the gravitational pull and radiation pressure are equal. The TOV equation connects four separate forces: gravitational force (F_g), hydrostatic force (F_h), anisotropic force (F_a) and Rastall gravity force (F_r). In terms of forces, above equation can be interpreted as

$$F_r+F_a+F_g+F_h=0, \tag{19}$$

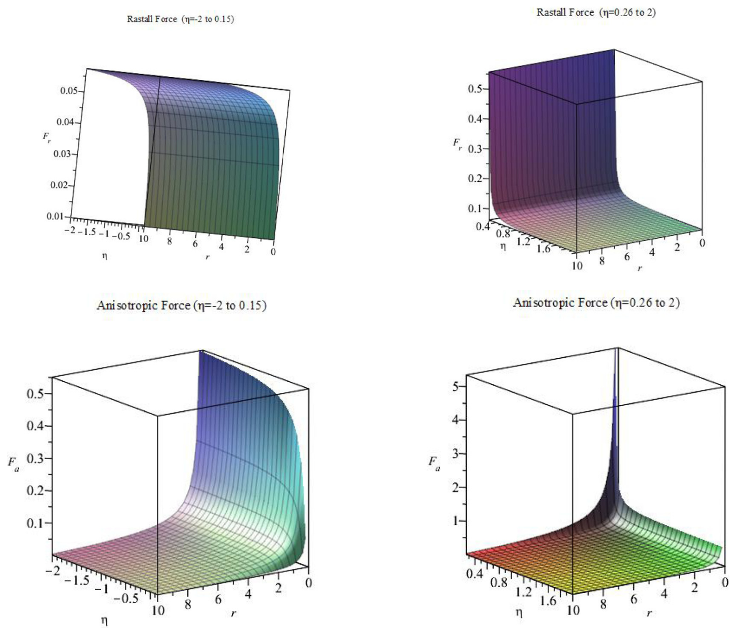

Fig. 13. Variation of Rastall, anisotropic, gravitational and hydrostatic forces with respect to radius r and Rastall's dimensionless parameter $\eta < \frac{1}{6}$ and $\frac{1}{4} > \eta$.

where

$$\text{Rastall force:}\quad F_r = \left(\frac{\eta}{4\eta - 1}\right)\frac{d}{dr}(\rho - 3p + \lambda), \tag{20}$$

$$\text{Anisotropic force:}\quad F_a = \frac{2}{r}\lambda, \tag{21}$$

$$\text{Gravitational force:}\quad F_g = -\frac{(\gamma)'}{2}(\rho + p), \tag{22}$$

$$\text{Hydrostatic force:}\quad F_h = -\frac{dp}{dr}. \tag{23}$$

The profile of these forces for the considered compact stars is shown in the following figures.

Figures 13 and 14 exhibit that Rastall, anisotropic, gravitational and hydrostatic forces vary corresponding to radial coordinate r and Rastall's dimensionless parameter η. Figure 13 presents the Rastall and anisotropic forces for the spherical configuration. It is exhibited that both these forces decrease with the increase in Rastall parameter η. The anisotropic force is inversely proportional to the radius. It gradually reduces with the increase in radius. Figure 14 shows gravitational and hydrostatic forces. It is worth mentioning that during collapse the gravitational force is negative and decreases gradually with the decrease in radius. Thus, it has

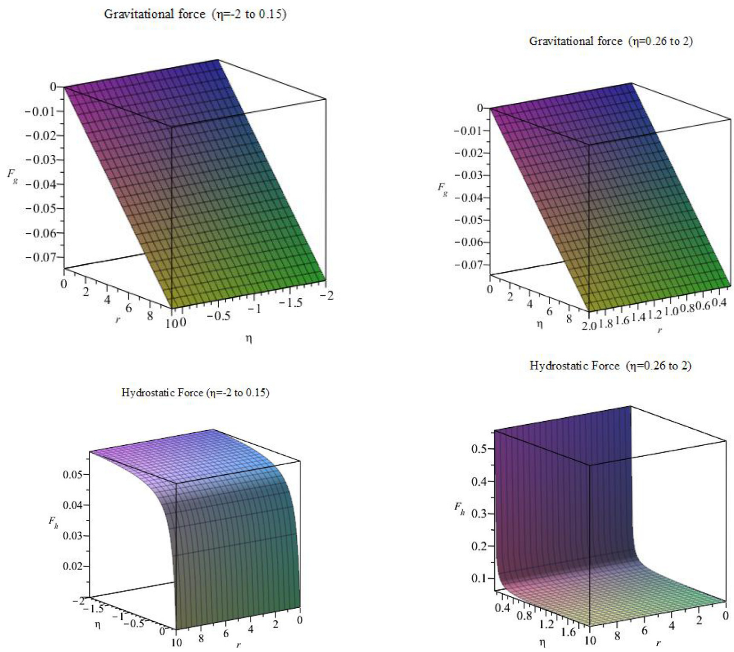

Fig. 14. Variation of Rastall, anisotropic, gravitational and hydrostatic forces with respect to radius r and Rastall's dimensionless parameter $\eta < \frac{1}{6}$ and $\frac{1}{4} > \eta$.

a repellent effect. However, the Rastall, anisotropic and hydrostatic forces have a combined positive effect which balances the gravitational force to leave stellar configuration in equilibrium state.

For the understanding point of view, the variation of Rastall, anisotropic, gravitational and hydrostatic forces are plotted against the radial coordinate r and Rastall parameter η for the three model compact stars SAX J1808.4-3658, Vela X-1 and Hercules X-1.

Figures 15–17 indicates all the four forces obtained from modified TOV equation corresponding to radial coordinate r and Rastall dimensionless parameter η for the mentioned compact stars candidates. The figures show that the gravitational, hydrostatic and Rastall forces decrease whereas the anisotropic force increases with the increase in Rastall's parameter η. However, the effect of gravitational force is equalized with the combined effect of Rastall, anisotropic and hydrostatic forces.

4.5. *Mass function and compactness*

The mass function of a collapsing dynamical system gives the mass of the configuration dependent on the radius. As the radius shortens due to collapse, the mass varies and gets compact. The mass function of a stellar configuration dependent on

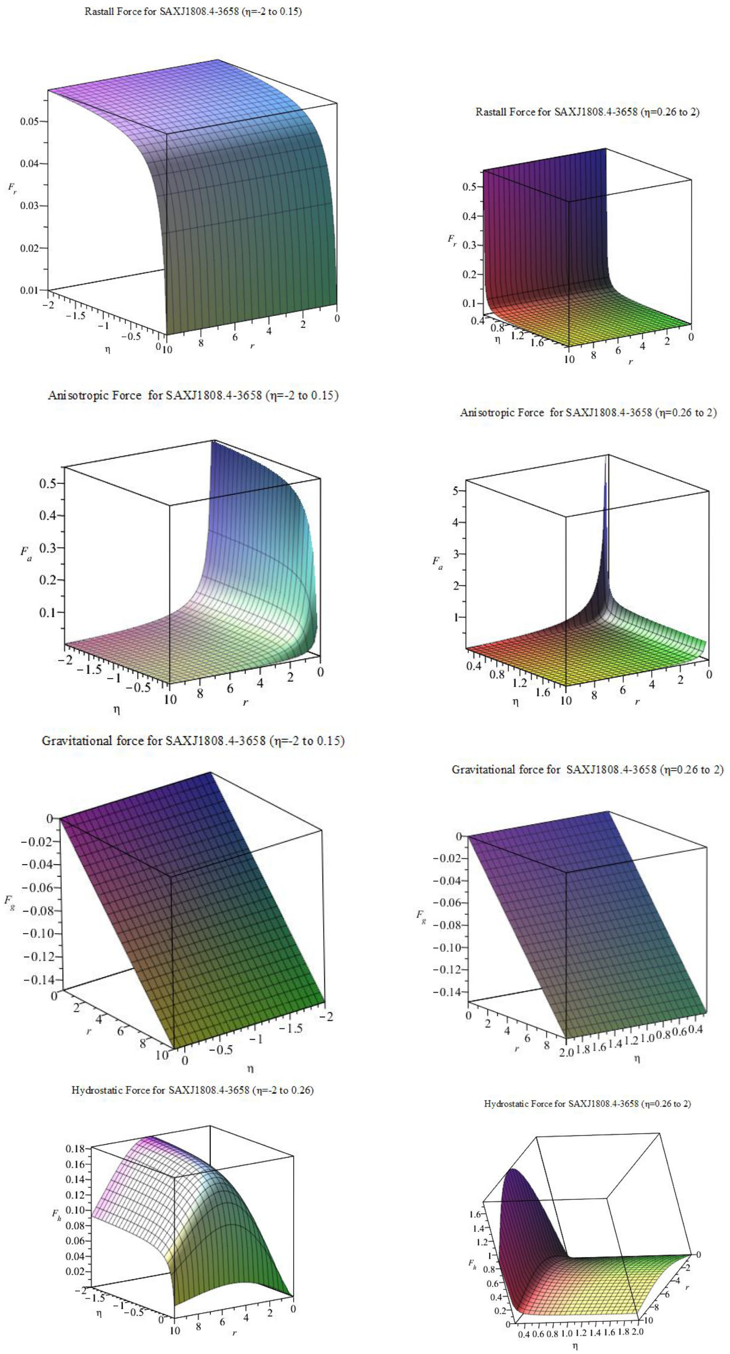

Fig. 15. Variation of different forces for compact star candidate SAX J1808.4-3658.

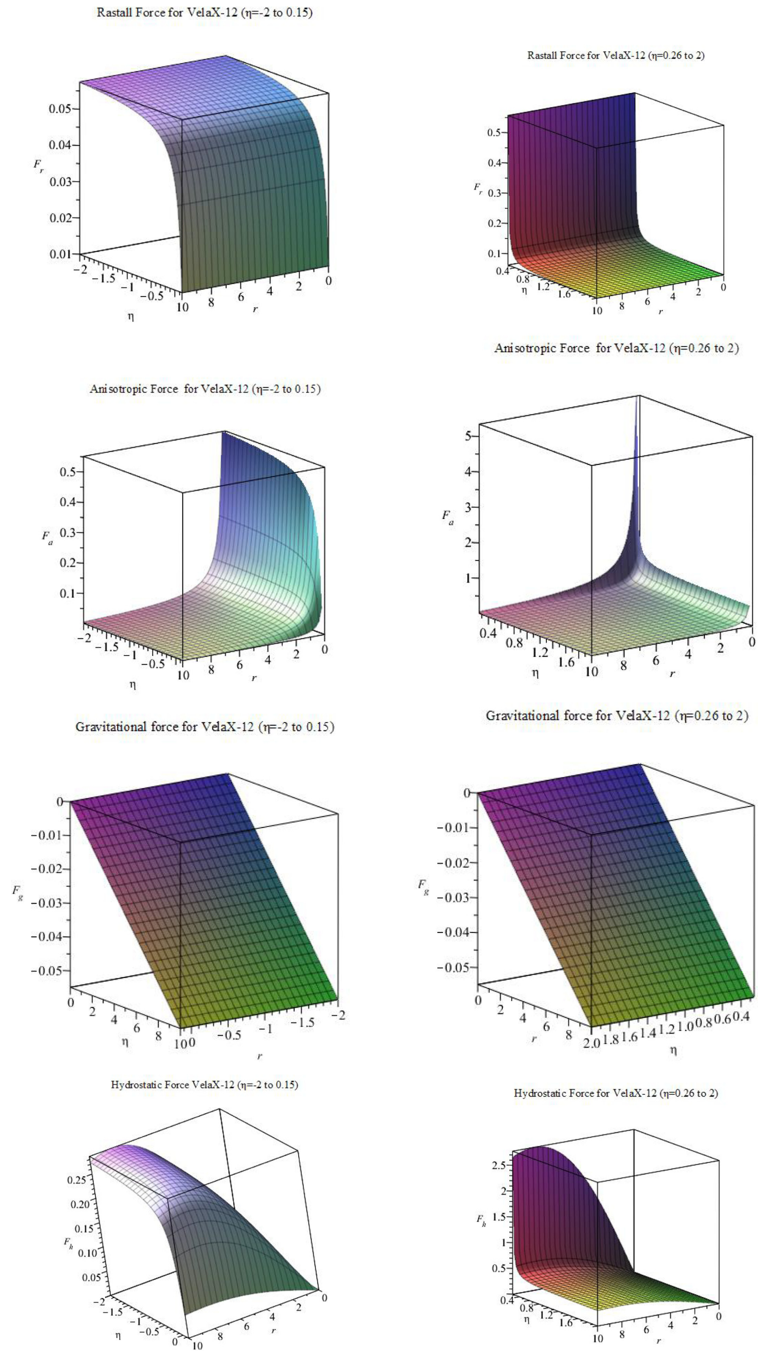

Fig. 16. Variation of different forces for compact star candidate Vela X-12.

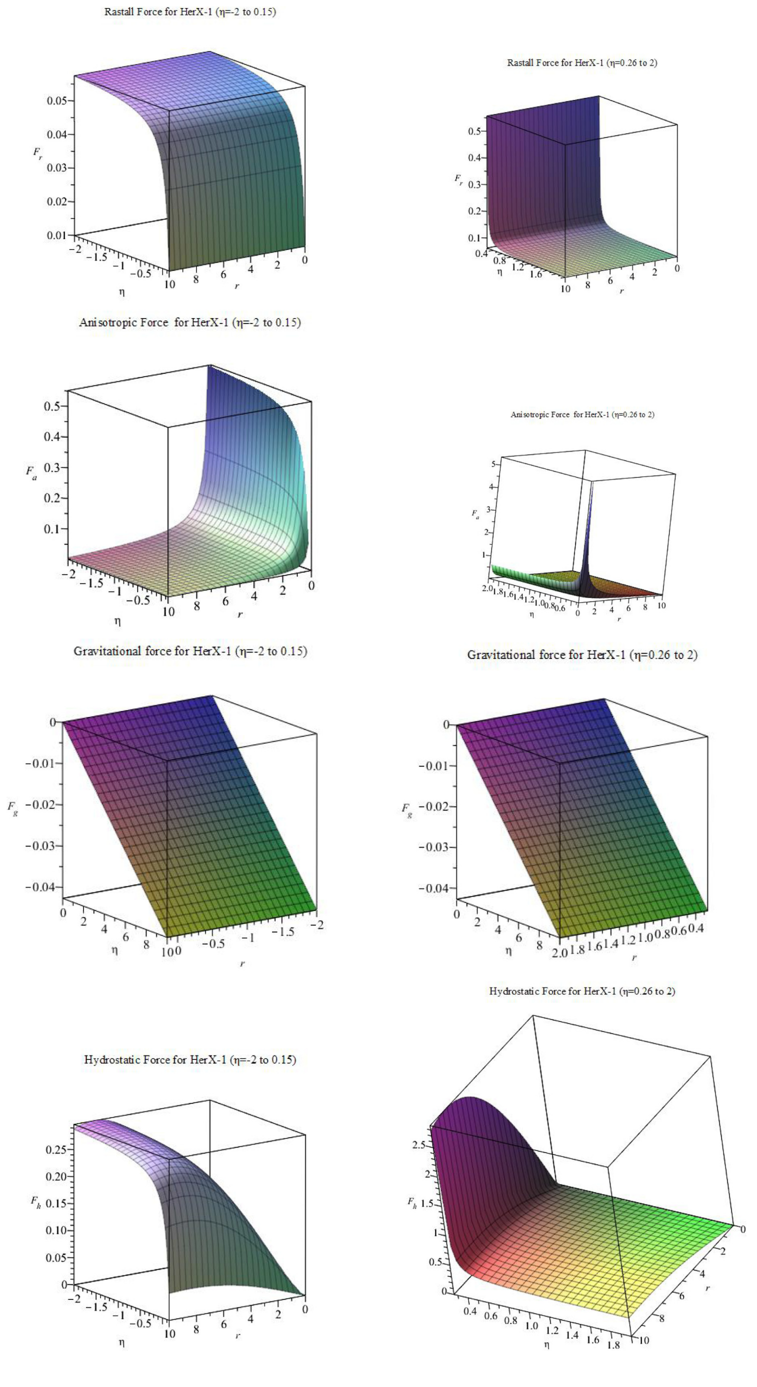

Fig. 17. Variation of different forces for compact star candidate Hercules X-1.

r is defined as [54]

$$M(r) = \int_0^r (4\pi r^2 \rho dr). \tag{24}$$

For the string fluid, this function takes the following form:

$$\begin{aligned} M(r) &= \frac{6\eta - 1}{4\eta - 1} \int_0^r \frac{r^2 e^{-Lr^2}}{2\pi} \left[\frac{e^{Lr^2} - 1}{r^2} + 2L + \eta \left\{ (2Q + 4Qr^2(Q - L) \right.\right. \\ &\quad \left.\left. - 4(L - Q) - \frac{2}{r^2}(e^{Lr^2} - 1) \right\} \right] dr \\ &= \frac{1}{2\pi} \left(\frac{6\eta - 1}{4\eta - 1} \right) \left[(1 - 2\eta) \left(r - \frac{\sqrt{\pi} erf(\sqrt{L} r)}{2\sqrt{L}} \right) + (2L - 2\eta(2L - 3Q)) \right. \\ &\quad \times \frac{-2re^{-Lr^2} L^{\frac{3}{2}} + \sqrt{\pi} L erf(\sqrt{L} r)}{4L^{\frac{5}{2}}} \\ &\quad \left. + 4\eta Q(Q - L) \left\{ \frac{-4r^3 e^{-Lr^2} L^{\frac{5}{2}} - 6re^{-Lr^2} L^{\frac{3}{2}} + 3\sqrt{\pi} L erf(\sqrt{L} r)}{8L^{\frac{7}{2}}} \right] \right.. \end{aligned} \tag{25}$$

The three-dimensional profile of mass function for a general model dependent on radius r is shown in Fig. 18.

It is evident that the mass function increases with the increase in r and decrease in the Rastall parameter η. The same behavior is exhibited in Fig. 19 for the three model compact objects SAX J1808.4-3658, Vela X-12 and Hercules X-1.

The compactness $u(r)$ of the stellar configuration is the ratio of mass M to the radius r of the configuration. For our fluid-containing model, the compactness can

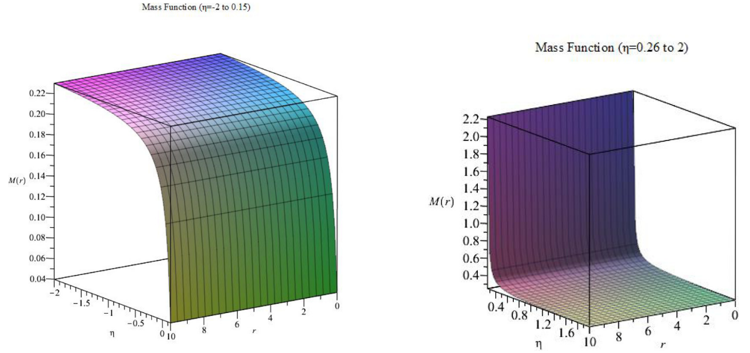

Fig. 18. Variation of mass function $M(r)$ with respect to radius r and Rastall's dimensionless parameter $\eta < \frac{1}{6}$ and $\frac{1}{4} > \eta$.

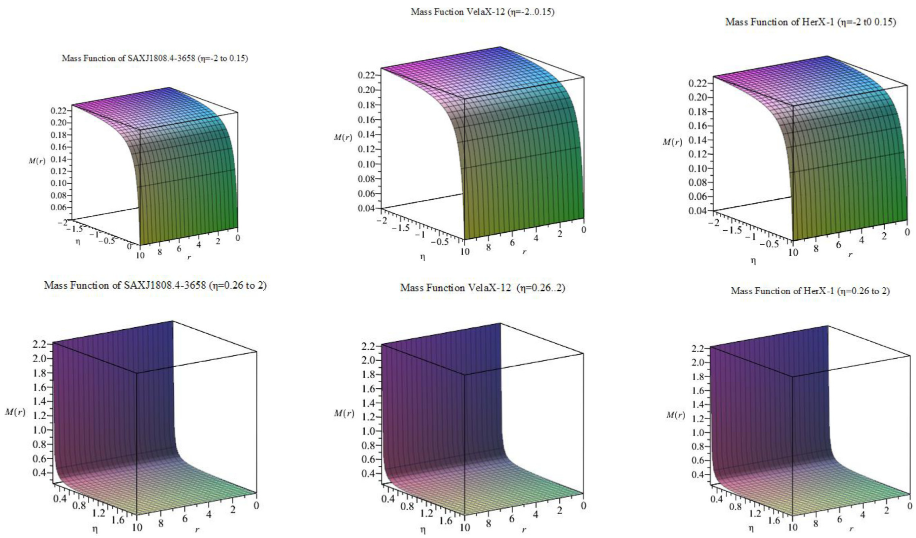

Fig. 19. Variation of the mass function $M(r)$ for compact star candidates SAX J1808.4-3658, Vela X-12 and Hercules X-1.

be computed as follows:

$$
\begin{aligned}
u(r) &= \frac{M}{R} \\
&= \frac{1}{2R\pi}\left(\frac{6\eta-1}{4\eta-1}\right)\left[(1-2\eta)\left(r-\frac{\sqrt{\pi}erf(\sqrt{L}r)}{2\sqrt{L}}\right)\right. \\
&\quad + (2L-2\eta(2L-3Q)) \times \frac{-2re^{-Lr^2}L^{\frac{3}{2}}+\sqrt{\pi}Lerf(\sqrt{L}r)}{4L^{\frac{5}{2}}} + 4\eta Q(Q-L) \\
&\quad \times \left\{\left.\frac{-4r^3e^{-Lr^2}L^{\frac{5}{2}}-6re^{-Lr^2}L^{\frac{3}{2}}+3\sqrt{\pi}Lerf(\sqrt{L}r)}{8L^{\frac{7}{2}}}\right]\right. .
\end{aligned}
\tag{26}
$$

The three-dimensional profile of compactness for a general star model is demonstrated in Fig. 20.

Figure 20 illustrates that compactness decreases with the increase in radius and Rastall parameter η. The same behavior is depicted from Fig. 21 for the three model compact objects SAX j1808.4-3658, Vela X-12 and Hercules X-1.

4.6. *Redshift*

The surface redshift is a phenomenon to interpret the dynamics of strong interaction between the internal distribution of star and its state. Corresponding to the above compactness factor $u(r)$, the surface redshift Z_s can be expressed as

$$Z_s = [1-2u(r)]^{-\frac{1}{2}} - 1.$$

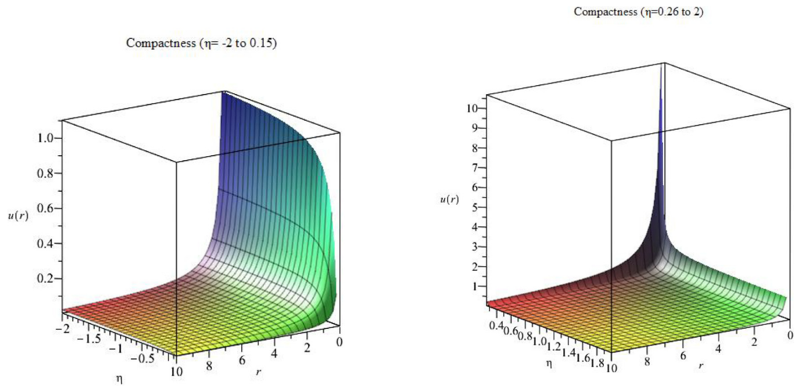

Fig. 20. Variation of compactness $u(r)$ with respect to radius r and Rastall's dimensionless parameter $\eta < \frac{1}{6}$ and $\frac{1}{4} > \eta$.

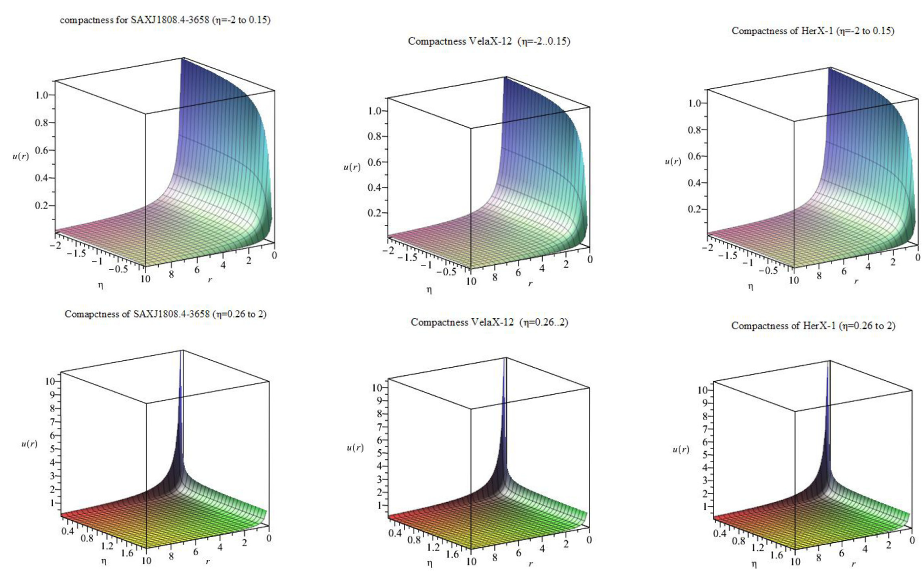

Fig. 21. Variation of compactness $u(r)$ for compact star candidates SAX J1808.4-3658, Vela X-12 and Hercules X-1.

The profile of the surface redshift against the radius r and Rastall parameter η is given in Fig. 22.

It is evident from the plots that Z_s takes the highest value of 16 due to anisotropy of the fluid. For isotropic matter configuration in the absence of cosmological constant, it is found that maximum value of surface redshift is $Z_s \leq 2$ [55]. Bohmer and Harko [56] insisted that the surface redshift becomes large, i.e. $Z_s \leq 5$ for an anisotropic star in the presence of a cosmological constant. Ivanov [57] argued

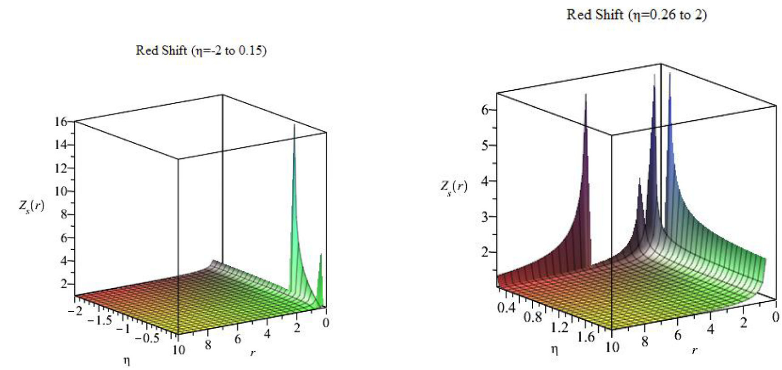

Fig. 22. Variation of Z_s with respect to radius r and Rastall's dimensionless parameter $\eta < \frac{1}{6}$ and $\frac{1}{4} > \eta$.

that $Z_s \leq 5.211$. Our model gives a much larger redshift, especially at $\eta = -0.4$. However, the model shows the maximum redshift of $Z_s \leq 6$ for the positive values of η. It is interesting to note that for the negative values of Rastall parameter, the maximum redshift is 16 at $\eta = -0.4$. Moreover, the redshift takes its maximum value near the center of the configuration $r = 0$. Thus, not only the string tension but the Rastall parameter η affects the measure of redshift. The same behavior is evident for each of the model compact stars including SAX J1808.4-3658, Vela X-12 and Hercules X-1 in Fig. 23.

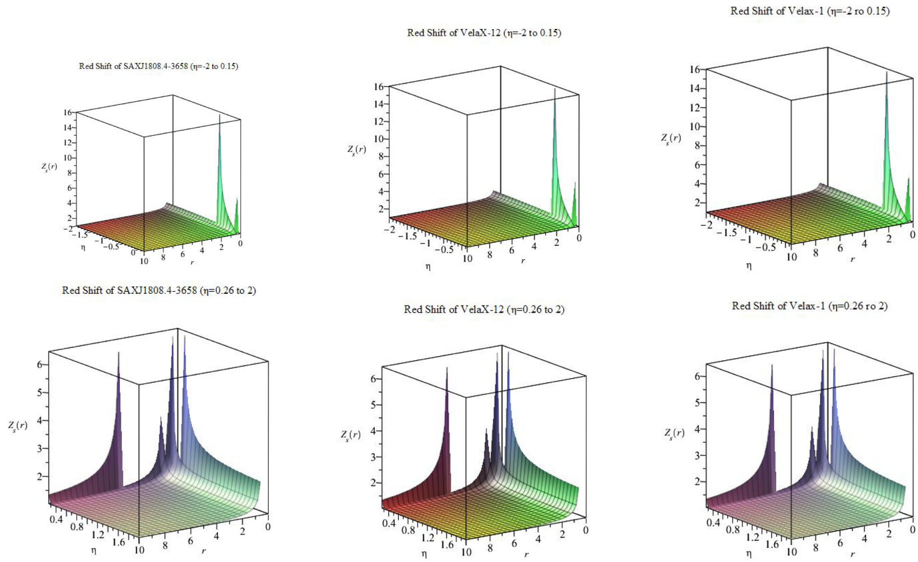

Fig. 23. Variation of Z_s for compact stars SAX J1808.4-3658, Vela X-12 and Hercules X-1.

5. Conclusion

This work models an anisotropic compact star as a result of string fluid collapse in Rastall's theory. The coefficients of KB ansatz are determined from interior KB metric and exterior Schwarzschild metric. The dynamical parameters are computed and the Rastall dimensionless parameter η is estimated for physical solution. This model is physically possible for $\eta < \frac{1}{6}$ and $\eta > \frac{1}{4}$. The model is applied on three distinct compact star candidates SAX J1808.4-3658, Vela X-12 and Hercules X-1 to investigate their physical features. The energy conditions, anisotropy, stability, TOV equation, mass function, compactness and redshift are analyzed. This research lead to the following results:

- It is found that the dynamical variables of a string fluid, collapsing to form a compact object, physically exist for the Rastall parameter $\eta < \frac{1}{6}$ and $\eta > \frac{1}{4}$. The case $\eta = 0$ leads to the general relativistic case which is also a physical one according to our study. Moreover, all the energy conditions are fulfilled for these values of Rastall parameter.
- It is verified that the KB ansatz satisfy the energy conditions for the three compact stars, i.e. SAX J1808.4-3658, Vela X-12 and Hercules X-1.
- The measure of anisotropy *Delta* is found to be physical for the general case as well as for the compact stars SAX J1808.4-3658, Vela X-12 and Hercules X-1. Moreover, positive anisotropy $\Delta > 0$ indicates a repulsive anisotropic force which allows the formulation of a massive configuration.
- The stability of a compact object formed from the string fluid is analyzed using the Herrera cracking condition. It is found that the speed of sound remains in the limits of stability, i.e. $[0, 1]$ for the general case as well as for three compact stars SAX J1808.4-3658, Vela X-12 and Hercules X-1.
- The TOV equation is found to be satisfied by the fluid model. This indicates a balance in Rastall, anisotropic, gravitational and hydrostatic forces leading to the static equilibrium of the configuration. It has been found that the repelling gravitational force is balanced by the Rastall, anisotropic and hydrostatic force.
- The mass function and compactness of the star model have been evaluated. Both these functions are inversely affected by the Rastall parameter.
- The surface redshift of the compact object is found to be the maximum at $\eta = -0.4$. At the rest of the values of the Rastall parameter, the surface redshift satisfies the results given in literature.

All the findings emphasize the possible existence of a spherically symmetric compact star evolve from a string fluid. It has been found that the Rastall parameter has an inverse effect on most of the physical attributes. The vanishing Rastall parameter leads to the general relativity case. The anisotropy of the string fluid leads to different properties compared to the previous literature. It is a strong theoretical observation for the evolution of compact stars from anisotropic string fluid.

There are hints that the Rastall theory may be a promising theory of gravity as it supports astrophysical objects with appealing behavior. Rastall claims that the non-conservation of energy–momentum is a consequence of spacetime curvature. The weak, strong and dominant energy criteria are satisfied by all values of the Rastall parameter, but this does not indicate that energy is conserved.

A mathematical solution to general relativity's flaws is provided by the Rastall parameter. The real theory of gravity is still a matter of debate. This study demonstrates that given this paradigm, it is simple to build astrophysical models that are physically sound. The significance is the accuracy with which this framework can produce solutions [60].

Acknowledgments

This work was partially funded by Slovak Grant Agency for Science VEGA under the grant number VEGA 2/0009/19. Moreover, the authors acknowledge the support of HEC Pakistan, National Textile University Faisalabad and University of Education, Lahore for their administrative and technical support.

References

[1] M. Sharif and A. Waseem, Stellar evolution of compact stars in curvature–matter-coupling gravity, *Prog. Theor. Exp. Phys.* **2019**(5) (2019) 053E02.

[2] M. Bhatti, Z. Yousaf and M. Ilyas, Evolution of compact stars and dark dynamical variables, *Eur. Phys. J. C* **77**(10) (2017) 1–9.

[3] S. Hansraj, A. Banerjee, L. Moodly and M. K. Jasim, Isotropic compact stars in 4D Einstein–Gauss–Bonnet gravity, *Class. Quantum Grav.* **38**(3) (2020) 035002.

[4] J. E. Delgado, J. V. Cabrera, J. A. R. Ceballos and J. M. P. Fuentes, An anisotropic model for represent compact stars, *Modern Phys. Lett. A* **35**(16) (2020) 2050132.

[5] A. C. Khunt, V. O. Thomas and P. C. Vinodkumar, Distinct classes of compact stars based on geometrically deduced equations of state, *Internat. J. Modern Phys. D* **30**(04) (2021) 2150029.

[6] P. Bhar, K. N. Singh and T. Manna, A new class of relativistic model of compact stars of embedding class I, *Internat. J. Modern Phys. D* **26**(9) (2017) 1750090.

[7] K. D. Krori and J. Barua, A singularity free solution for a charged fluid sphere in general relativity, *J. Phys. A* **8**(4) (1975) 508–511.

[8] S. Biswas, S. Ghosh, B. K. Guha, F. Rahaman and S. Ray, Strange stars in Krori–Barua space-time under $f(R,T)$ gravity, *Ann. Phys.* **401** (2019) 1–20.

[9] P. Rastall, Generalization of the Einstein theory, *Phys. Rev. D* **6**(12) (1972) 3357–3359.

[10] F. Darabi, H. Moradpour, I. Licata, Y. Heydarzade and C. Corda, Einstein and Rastall theories of gravitation in comparison, *Eur. Phys. J. C* **78** (2018) 25–28.

[11] R. Rizaldy and A. Sulaksono, Deformation of a magnetized quark star in Rastall gravity, *J. Phys. Conf. Ser.* **1321** (2019) 022016.

[12] F. M. da Silva, L. C. N. Santos and C. C. Barros Jr., Rapidly rotating compact stars in Rastall's gravity, *Class. Quantum Grav.* **38**(16) (2021) 165011.

[13] M. R. Shahzad and G. Abbas, Models of quintessence compact stars in Rastall gravity consistent with observational data, *Eur. Phys. J. Plus* **135**(6) (2020) 1–17.

[14] M. R. Shahzad and G. Abbas, Strange stars with MIT bag model in the Rastall theory of gravity, *Int. J. Geom. Methods Modern Phys.* **16**(9) (2019) 1950132.
[15] M. F. Shamir and I. Fayyaz, Effect of $f(R)$-gravity models on compact stars, *Theoret. Math. Phys.* **202**(1) (2020) 112–125.
[16] M. Sharif and M. Aslam, Compact objects by gravitational decoupling in $f(R)$ gravity, *Eur. Phys. J. C* **81**(7) (2021) 641.
[17] T. Naz, A. Usman and M. F. Shamir, Embedded class-I solution of compact stars in $f(R)$ gravity with Karmarkar condition, *Ann. Phys.* **429** (2021) 168491.
[18] G. G. L. Nashed, Rotating charged black hole spacetimes in quadratic $f(R)$ gravitational theories, *Internat. J. Modern Phys. D* **27**(07) (2018) 1850074.
[19] M. Bandyopadhyay and R. Biswas, Repulsive gravitational force and quintessence field in $f(T)$ gravity: How anisotropic compact stars in strong energy condition behave, *Modern Phys. Lett. A* **36**(7) (2021) 150044.
[20] Z. Yousaf, M. Z. Bhatti and M. Ilyas, Existence of compact structures in $f(R,T)$ gravity, *Eur. Phys. J. C* **78**(4) (2018) 1–13.
[21] K. N. Singh, A. Errehymy, F. Rahaman and M. Daoud, Exploring physical properties of compact stars in $f(R,T)$-gravity: An embedding approach, *Chin. Phys. C* **44**(10) (2020) 105106.
[22] S. Biswas, D. Shee, S. Ray and B. K. Guha, Anisotropic strange star with Tolman–Kuchowicz metric under $f(R,T)$ gravity, *Eur. Phys. J. C* **80** (2020) 175.
[23] M. F. Shamir and T. Naaz, Stellar structures in $f(G)$ gravity with Tolman–Kuchowicz spacetime, *Phys. Dark Universe* **27** (2020) 100472.
[24] M. Z. Bhatti, M. Y. Khlopov, Z. Yousaf and S. Khan, Electromagnetic field and complexity of relativistic fluids in $f(G)$ gravity, *Mon. Not. R. Astron. Soc.* **506**(3) (2021) 4543–4560.
[25] G. Mustafa, X. Tie-Cheng and M. F. Shamir, Realistic solutions of fluid spheres in $f(G,T)$ gravity under Karmarkar condition, *Ann. Phys.* **413** (2020) 168059.
[26] M. Z. Bhatti and Z. Tariq, Effects of electromagnetic field on the structure of massive compact objects, *Phys. Dark Universe* **29** (2021) 100600.
[27] I. G. Salako, M. Khlopov, S. Ray, M. Z. Arouko, P. Saha and U. Debnath, Study on anisotropic strange stars in $f(T,T)$ gravity, *Universe* **6**(10) (2020) 167.
[28] T. Shirafuji and G. G. L. Nashed, Energy and momentum in the tetrad theory of gravitation, *Progr. Theoret. Phys.* **98**(6) (1997) 1355–1370, arXiv: gr-qc/9711010.
[29] G. G. L. Nashed, Charged axially symmetric solution, energy and angular momentum in tetrad theory of gravitation, *Internat. J. Modern Phys. A* **21**(15) (2006) 3181–3197, arXiv: gr-qc/0501002.
[30] A. Awad, W. El Hanafy, G. G. L. Nashed, S. D. Odintsov and V. K. Oikonomou, Constant-roll inflation in $f(T)$ teleparallel gravity, *J. Cosmol. Astropart. Phys.* **2018**(07) (2018) 026, arXiv: 1710.00682.
[31] E. Elizalde, G. G. L. Nashed, S. Nojiri and S. D. Odintsov, Spherically symmetric black holes with electric and magnetic charge in extended gravity: Physical properties, causal structure, and stability analysis in Einstein's and Jordan's frames, *Eur. Phys. J. C* **80**(2) (2020) 1–23, arXiv: 2001.11357.
[32] A. Awad and G. Nashed, Generalized teleparallel cosmology and initial singularity crossing, *J. Cosmol. Astropart. Phys.* **2017**(02) (2017) 046, arXiv: 1701.06899.
[33] G. G. L. Nashed, Brane world black holes in teleparallel theory equivalent to general relativity and their Killing vectors, energy, momentum and angular momentum, *Chin. Phys. B* **19**(2) (2010) 020401, arXiv: 0910.512.

[34] G. G. L. Nashed, Energy and momentum of a spherically symmetric dilaton frame as regularized by teleparallel gravity, *Ann. Phys.* **523**(6) (2011) 450–458, arXiv: 1105.0328.
[35] G. G. L. Nashed, Schwarzschild solution in extended teleparallel gravity, *Europhys. Lett.* **105**(1) (2014) 10001.
[36] G. G. L. Nashed and W. El Hanafy, Analytic rotating black-hole solutions in N-dimensional $f(T)$ gravity, *Eur. Phys. J. C* **77**(2) (2017) 1–9, arXiv: 1612.0510.
[37] W. El Hanafy and G. G. L. Nashed, Exact teleparallel gravity of binary black holes, *Astrophys. Space Sci.* **361**(2) (2016) 1–11.
[38] G. G. L. Nashed and E. N. Saridakis, Rotating AdS black holes in Maxwell-$f(T)$ gravity, *Class. Quantum Grav.* **36**(13) (2019) 135005, arXiv: 1811.03658.
[39] M. Sharif and A. Majid, Decoupled embedding class-one strange stars in self-interacting Brans–Dicke gravity, *Universe* **7**(6) (2021) 161.
[40] N. Nari and M. Roshan, Compact stars in energy–momentum squared gravity, *Phys. Rev. D* **98**(2) (2018) 024031.
[41] U. Sheikh, K. Mahmood and M. Arshad, Analysis of a charged unidirectional perfect fluid gravitational collapse in cylindrical spacetime, *Chin. J. Phys.* **73** (2021) 503–511.
[42] U. Sheikh, S. Liaqut, Z. Yousaf and M. Z. Bhatti, Information paradox for a collapsing string cloud in rainbow gravity, *Int. J. Geom. Methods Mod. Phys.* **18**(06) (2021) 2150084.
[43] U. Sheikh, S. Arshad and M. Arshad, Dynamics of charged string cloud collapse in rainbow gravity, *Int. J. Geom. Methods Mod. Phys.* **19**(12) (2022) 2250185.
[44] U. Sheikh and S. Arshad, Electromagnetic effects on dynamics of string fluid and information paradox in rainbow gravity, *Ann. Phys.* **441** (2021) 168855.
[45] U. Sheikh, Z. Yousaf and N. Ramzan, On dynamical stability and information loss of collapsing string fluid in rainbow gravity, *Modern Phys. Lett. A* (2022).
[46] S. D. Maharaj and B. P. Brassel, Radiating composite stars with electromagnetic fields, *Eur. Phys. J. C* **81**(9) (2021) 783.
[47] S. D. Maharaj and B. P. Brassel, Radiating stars with composite matter distributions, *Eur. Phys. J. C* **81**(4) (2021) 366.
[48] A. Z. Jones, *String Theory for Dummies* (John Wiley and Sons, 2009).
[49] P. Bhar, A new hybrid star model in Krori–Barua spacetime, *Astrophys. Space Sci.* **357** (2015) 46.
[50] G. Abbas and M. R. Shahzad, A new model of quintessence compact stars in the Rastall theory of gravity, *Eur. Phys. J. A* **54** (2018) 211.
[51] G. Abbas and M. R. Shahzad, Models of anisotropic compact stars in the Rastall theory of gravity, *Astrophys. Space Sci.* **364**(50) (2019) 1–12.
[52] L. Herrera, Cracking of self-gravitating compact objects, *Phys. Lett. A* **165**(3) (1992) 206–210.
[53] C. E. Rhoades Jr. and R. Ruffini, Maximum mass of a neutron star, *Phys. Rev. Lett.* **32**(6) (1974) 324.
[54] P. Bhar, Higher dimensional charged gravastar admitting conformal motion, *Astrophys. Space Sci.* **354**(2) (2014) 457–462.
[55] C. G. Bohmer and T. Harko, Minimum mass–radius ratio for charged gravitational objects, *Gen. Relativ. Gravit.* **39** (2007) 757–775.
[56] C. G. Bohmer and T. Harko, Bounds on the basic physical parameters for anisotropic compact general relativistic objects, *Class. Quantum Grav.* **23** (2006) 6479–6491.
[57] B. V. Ivanov, Maximum bounds on the surface redshift of anisotropic stars, *Phys. Rev. D* **65**(10) (2002) 104011.

[58] R. C. Tolman, Static solutions of Einstein's field equations for spheres of fluid, *Phys. Rev.* **55** (1939) 364–373.
[59] J. R. Oppenheimer and G. M. Volkoff, On massive neutron cores, *Phys. Rev.* **55** (1939) 374–381.
[60] S. Hansraj, B. Ayan and P. Channuie, Impact of the Rastall parameter on perfect fluid spheres, *Ann. Phys.* **400** (2019) 320–345.